
Validation of MERIT DEM's Performance as a Bare-Earth Model Using ICESat-2 Geolocated Photons

Giribabu Dandabathula^{1,*}, Rohit Hari¹, Jayant Sharma², Koushik Ghosh¹, Apurba Kumar Bera¹

¹Regional Remote Sensing Centre, National Remote Sensing Centre / Indian Space Research Organisation, Jodhpur, India

²School of Computer Application, Jaipur Engineering College and Research Centre (JECRC) University, Jaipur, India

Email address:

dgb.isro@gmail.com (Giribabu Dandabathula)

*Corresponding author

To cite this article:

Giribabu Dandabathula, Rohit Hari, Jayant Sharma, Koushik Ghosh, Apurba Kumar Bera. Validation of MERIT DEM's Performance as a Bare-Earth Model Using ICESat-2 Geolocated Photons. *Earth Sciences*. Vol. 12, No. 5, 2023, pp. 166-175. doi: 10.11648/j.earth.20231205.15

Received: September 19, 2023; **Accepted:** October 8, 2023; **Published:** October 14, 2023

Abstract: Digital elevation models represent the Earth's surface and play a key role in earth sciences by enabling the possibility of deriving terrain variables; the terrain variables are essential inputs for environmental modeling. The availability of open-access digital surface models has significantly advanced the understanding of earth system dynamics and also allowed researchers to generate digital terrain models, aka bare-earth models. These bare-earth models are essential data sets for applications related to hydrology and geomorphology, especially for disaster management. Under the category of open-accessible bare-earth models, Multi-Error-Removed Improved-Terrain DEM or MERIT DEM is the first kind of product unfolded by applying numerous error removal algorithms from existing DEM sources. This research reports the results after validating the MERIT DEM's performance by emphasizing its tree-height bias removal algorithm. Towards this, ground-reflected photons accrued from the ICESat-2 mission were used as reference data due to their attribution of high accuracy. Two test sites, one located in the rugged terrain of the outer Himalayas, the Lacchiwala Reserve forest, and the other, rolling hills at the Bhadra wildlife sanctuary located in the Western Ghats of the Indian sub-continent were used as test sites for validating the MERIT DEM's accuracy. The results derived after computing statistical formulae like RMSE, MAE, MBE, and profile-based visual analytics helped understand the performance of the MERIT DEM as a bare-earth model. The RMSE, MAE, and MBE for the Lachhiwala Reserve forest are 10.28 m, 7.78 m, and 0.69 m, respectively. Similarly, the RMSE, MAE, and MBE values for the Bhadra wildlife sanctuary are 4.52 m, 3.82 m, and 3.04 m, respectively. The assessment confirms that the accuracies are within the MERIT DEM's specifications and assured the successful implementation of MERIT DEM's tree-height removal algorithm since the elevations from the MERIT DEM are always lesser than the canopy height in both the test sites. Our research also investigated the reasons for the inaccuracies obtained at both the test sites and suggested using improved tree-height estimations from high-resolution canopy height data in the future version of MERIT DEM.

Keywords: MERIT DEM, Bare-Earth Model, ICESat-2, Geolocated Photons, Accuracy Assessment, Tree-Height Bias

1. Introduction

A Digital Elevation Model (DEM) represents a digital format of equally spaced grid cells containing terrain elevation values over a given area [1]. DEMs are the most commonly used data in environment simulation models, primarily for applications that deal with hydrology. Space-borne Earth observation missions like Shuttle Radar Topography Mission (SRTM), Advanced Space-borne Thermal Emission and Reflection Radiometer (ASTER),

Advanced Land Observing Satellite (ALOS), and TerraSAR-X add-on for Digital Elevation Measurements (TANDEM-X) have enabled the generation of DEMs at the global level. These DEMs recently gained tremendous popularity among the scientific fraternity and helped to advance the understanding of Earth sciences. However, these DEMs include inaccuracies and model errors (namely voids, spikes, sinks, and artifacts) that resulted from various phases of the DEM generation process, from data acquisition to model computation [2-4]. Moreover, space-borne-based DEMs include elevation biases from the vegetation canopy

and man-made structures that result in a Digital Surface Model (DSM), i.e., adding a positive offset to the true bare-earth model or a Digital Terrain Model (DTM). Post-processing efforts can help reduce model errors [5]. However, regenerating a bare-earth model from existing DSM requires systematic removal of height offsets due to canopy and man-made structures. Sampson *et al.* argue that current open-access global DEMs need improvement using further advancements [6]; otherwise, they are not qualified to derive important hydrological parameters from them.

Recently, efforts have been underway to generate a true bare-earth model from existing open-access global DEMs by using lidar point clouds and machine learning methods [7-13]. Multi-Error-Removed Improved Terrain (MERIT) DEM was generated by applying a global-scale error-removal algorithm using the existing space-borne DEMs like SRTM and ALOS World 3D DEM (AW3D DEM) by Yamazaki *et al.* [14]. MERIT DEM is being disseminated to the scientific fraternity as open-access at 3 arc-second (90 m). While developing the MERIT DEM, Yamazaki *et al.* enforced a four-step method for separating and removing the four major error components in space-borne DEMs; specifically, the errors are speckle noise, stripe noise, absolute bias, and bias due to tree heights [14]. Amatulli *et al.* [15] successfully utilized MERIT DEM to develop global high-resolution geomorphometric layers, during which MERIT DEM was credited as the best effort in global DEMs available to date.

Earlier, a global DEM was generated with a spatial resolution of 0.4 arc-seconds (12 m at the equator) from TanDEM-X, an Earth observation radar mission that consists of a SAR interferometer [16, 17]. Another global DEM, namely Copernicus DEM, was generated at 30 m resolution with open access provision using TanDEM-X [18]. By applying machine learning methods on Copernicus DEM, an elevation dataset titled Forest And Buildings removed Copernicus DEM (FABDEM) was generated by Hawker *et al.* which is made available as free and open-access at 1 arc-second (~30 m) grid spacing [13]. MERIT DEM and FABDEM are credited as bare-earth models that are available with open-access facilities and are preferred for many applications where a DTM is needed, such as hydrology and geomorphology.

Assessment of DEM's accuracy, specifically vertical accuracy, is crucial and requires to be examined before its practical usage. To validate the high-resolution DEM's vertical accuracy, comparing the heights retrieved from the DEM and the field measurements (termed reference points) obtained from a Global Position System (GPS) based survey is standard practice. During this comparison, quantification of the vertical error is done using statistical formulae like Root Mean Square Error (RMSE), Mean Absolute Error (MAE), and Mean Bias Error (MBE). RMSE shows how far predictions fall from measured true values using Euclidean distance and penalizes the larger errors more [19]. In MAE, errors are not weighted more or less, but the scores increase linearly with the increase in errors; however, the average of the absolute error values makes the statistical value always positive [20]. Like MAE, MBE also captures the average bias

in the prediction but has an advantage in determining whether the model is overestimating or underestimating. Usually, the area in the DEM where accuracy is high will yield lesser RMSE and MAE values. More information regarding the statistical evaluation methods of the DEM can be found at [21, 22].

However, the DEM's vertical accuracy assessment using the heights from a GPS-based survey poses certain limitations due to the limited number of reference points. The distribution of the reference points in the area of interest also matters during the evaluation process. Moreover, the GPS-based survey needs planned and rigorous fieldwork followed by post-processing [23]. To overcome these limitations and also, due to the advantage of high accuracy, height information from LiDAR-based acquisitions is suggested as reference data to evaluate a DEM [24-28]. Importantly, using a set of sparse reference points is not scientifically viable if dealing with 30 m or 90 m grid-spaced DEMs, especially in undulating terrains, because a single point cannot judge the spatial variations in the height represented by a grid cell. Dandabathula *et al.* have suggested using profiles derived from lidar-based acquisitions to overcome this; moreover, profile-based evaluation methods have an advantage in detecting errors at slopes [27]. The recent NASA space-based laser altimetry mission, the Ice, Cloud, and land Elevation Satellite - 2 (ICESat-2), hosts a solo sensor, namely, Advanced Topographic Laser Altimeter System (ATLAS) [29]. ATLAS sensor has the capability of multi-beam, a smaller footprint, and a fast-firing laser that yields geolocated photons, which are proven to be highly accurate elevation measurements [30]. A successful surface-reflected photon event counted by the ATLAS sensors results in the accumulation of geolocated photon data, primarily comprising attributes like height above the ellipsoid, time, latitude, and longitude. The trend to evaluate a DEM using ICESat-2 geolocated photon data has proven much more effective in understanding DEM quality [24, 26-28].

Previously, Bhardwaj [31], Dandabathula *et al.* [27], and Xu *et al.* [32] have evaluated FABDEM's tendency of a bare-earth model and concluded that it is a beneficial data resource for disaster-related applications, especially for flood hazard zonation and hydraulic simulations. Similarly, the performance of MERIT DEM and other open-access global DEMs was evaluated by various researchers [2, 4, 5, 33, 34, 35, 36]. The results from their investigations concluded that primarily, the algorithms implemented by Yamazaki *et al.* [9] to reduce the errors from SRTM were successful and evident in the form of MERIT DEM. Archer *et al.* [37], Xu *et al.* [38], Garrote [39], and Nguyen *et al.* [40] have evaluated the MERIT DEM in the context of hydrological applications; their results show that MERIT DEM's performance is nearly normal and errors are in the predictable limit. Chen *et al.* [26] tested the performance of MERIT DEM in the glacierized Tibetan Plateau; their results conclude that NASADEM is superior in performance compared with MERIT DEM. Maung and Sasaki [41] have assessed the natural recovery of mangroves after human disturbance using neural network classification and Sentinel-2 imagery in Wunbaik Mangrove

Forest, Myanmar. During this study, the authors found the topographic information derived from the MERIT DEM to be of utmost benefit; however, the coarse resolution of the MERIT DEM is a known hindrance.

In this study, we have validated the performance of MERIT DEM by emphasizing the forest regions. Yamazaki et al. [9], to generate a bare-earth model from the SRTM3 and AW3D DEMs, have included algorithms to reduce the bias accumulated due to the heights from the forest canopy and generated the MERIT DEM. Our study attempts to assess the nearness of MERIT DEM's bare-earth feature in the test sites of forest regions in the Indian subcontinent by utilizing the ground-reflected photons from ICESat-2 as reference data.

2. Material and Methods

2.1. Study Area

Two study areas falling in different elevation zones of the

Table 1. Summary of the study area and associated geospatial data that were used to investigate the accuracy assessment of MERIT DEM.

Study area	Dominant species and the range of tree height	ICESat-2 photon data details
Lachhiwala Reserve forest	Shorea robusta and ~33-35 m	gt31 (strong) acquired on 19 May 2020
Bhadra wildlife sanctuary	Albizia lebbek and ~20-25 m	gt21 (strong) acquired on 24 Feb. 2019

2.2. MERIT DEM

The MERIT DEM is open access and hosted by the University of Tokyo. One can download it at http://hydro.iis.u-tokyo.ac.jp/~yamadai/MERIT_DEM/ (registration required). By default, MERIT DEM tiles are arranged at 30 deg * 30 deg in GeoTiff format. The tile with id as dem_tif_n00e060 corresponding to both the study areas was downloaded for this research. Figure 1.d and 1.e shows the extent of the MERIT DEM for both the study areas, i.e., Lachhiwala Reserve forest and part of Bhadra wildlife sanctuary, with an overlay of subsets of ICESat-2 photon data. The details of ICESat-2 photon data are mentioned in the subsequent section.

2.3. ICESat-2 Photon Data

ICESat-2 provides several data products to the scientific fraternity; among these products, the Level 2A data product, identified as ATL03, provides the ancillary metadata during the photon event detection by the ATLAS instrument along with the latitude, longitude, and ellipsoidal height of photons [45]. The science teams of ICESat-2 apply advanced algorithms on ATL03 to produce higher-level surface-specific (glacier and ice sheet height, sea ice freeboard, vegetation canopy height, ocean surface topography, and inland water bodies) data products. All these products, including ATL03, are made open-access by the ICESat-2 team and hosted at <https://nsidc.org/data/icesat-2>. For this research, a subset of ATL03 data for a track stretch of 7.5 km was downloaded for each study area. The 7.5 km stretch enables to validation of nearly 83 grid cells of the MERIT DEM. Figure 1.b and 1.c shows the subsets of ATL03 (geolocated photons) overlaid on

Indian sub-continent were chosen for this research. Lachhiwala Reserve forest, a subtropical deciduous biodiversity-rich forest located in the Shivalik hills of the Himalayas with elevations ranging between 500 and 900 m.a.s.l, is the first study area. The part of this forest under investigation is a high abundance of Sal trees (*Shorea robusta* Roth.) as the dominant overstorey species with an average tree height of ~33 m [42, 43]. The second study area, Narasimharajpura forest block, a dry deciduous type on rolling hills (with a topographic variation of 600-700 m), is a part of the Bhadra wildlife sanctuary in the Western Ghats of the Indian subcontinent. The area is predominantly occupied by *Albizia lebbek* (the common name being women's tongue) species that have grown to a height of 22-25 m. More information about the study area and species details can be found in [44]. Table 1 shows the summary of the study areas along with relevant details. Figure 1a shows the map depicting the locations of the two study areas.

high-resolution imagery for the study areas, viz., the Lachhiwala Reserve forest and Bhadra wildlife sanctuary, respectively. We ensured that both the subsets of ATL03 photon data were acquired during night-time, and only strong beams were considered in this validation process. The rationale for this selection is attributed to the reason that night-time data and strong beams are less affected by atmospheric scattering and also have reduced solar background noise [20, 46].

2.4. Methodology

Although the ATLAS sensor of ICESat-2 is not designed for canopy-related applications, various researchers have successfully demonstrated that photon data from ICESat-2 can provide valuable information about the canopy height in forests [30, 47-49]. Various methods to separate the ICESat-2 photons reflected from the canopy and ground were discussed in [49].

Clustering is a process of unsupervised classification of patterned data into groups; it enables one to divide the whole set of data points into segregated groups such that each group contains data points of more similarity [50]. Clustering algorithms can be partition-based, hierarchical-based, density-based, and grid-based, as Mann and Kaur discussed [51]. Density-Based Spatial Clustering of Applications with Noise (DBSCAN), proposed by Ester et al. [52], is a widely used technique for class identification when there is limited knowledge concerning the input parameters [53]. Xie et al. [54] and Dandabathula et al. [27] suggested using unsupervised classification techniques like DBSCAN to separate the canopy and ground-reflected photons. Huang et al. [55] suggested using a localized statistical algorithm to improve the segregation of canopy-reflected and ground-reflected photons.

In our research, we used the DBSCAN algorithm to classify the canopy-reflected and ground-reflected photons; however,

photons reflected from the understory were removed by applying a localized statistical algorithm.

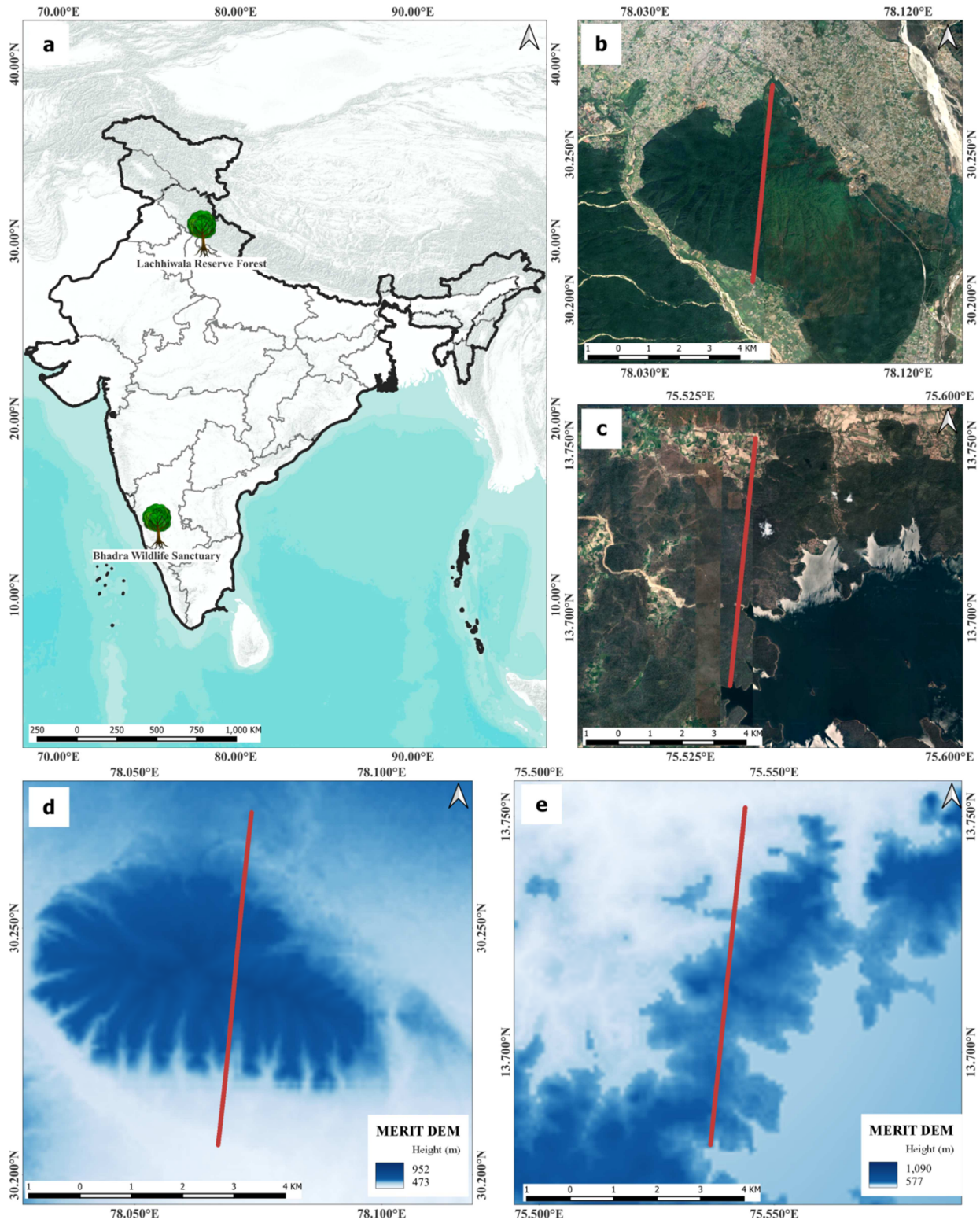


Figure 1. Test sites and geospatial data utilized in validating the MERIT DEM's performance in forest regions. *a* Map of India showing the two test site locations of this research. Source of shaded relief map: Hill-shade view of MERIT DEM. *b* Subset of ICESat-2's beam overlaid on high-resolution satellite imagery for the extent of the Lacchiwala Reserve forest. *c* Subset of ICESat-2's beam overlaid on high-resolution imagery for the extent of the Bhadra wildlife sanctuary. *d* Subset of ICESat-2's beam overlaid on MERIT DEM's shaded relief for the extent of the Lachhiwala Reserve forest. *e* Subset of ICESat-2's beam overlaid on MERIT DEM's shaded relief for the extent of the Bhadra wildlife sanctuary. Accessibility details of the MERIT DEM and ICESat-2 data were given in the Data availability section of this article. The source of high-resolution imagery in *b* and *c* are from the WMS service retrieved from bhuvan.nrsc.gov.in.

The vertical datum of the elevations from ICESat-2 ground reflected photons were converted from WGS84 ellipsoidal heights to the EGM96 geoid model; this was done to harmonize the comparison with the elevation values retrieved from MERIT DEM, which are in EGM96 geoid model. The EGM96 geoid heights grid can be obtained from <https://earth-info.nga.mil/index.php?dir=wgs84&action=wgs84>. Finally, to assess the accuracy of MERIT DEM, the elevation values from both the ICESat-2 ATL03 ground reflected photons and MERIT DEM were used to compute the RMSE and MAE using the below formulas.

$$\Delta H = Elevations_{ICESat-2} - Elevations_{MERIT\ DEM} \quad (1)$$

$$RMSE = \sqrt{\frac{\sum \Delta H^2}{n}} \quad (2)$$

$$MAE = \frac{\sum abs(\Delta H)}{n} \quad (3)$$

$$MBE = \frac{1}{n} \sum \Delta H \quad (4)$$

Where, $Elevation_{ICESat-2}$ is the set of height values obtained from the ICESat-2 ground-only reflected geolocated photons that are used as reference values, $Elevation_{MERIT\ DEM}$ is the height values retrieved from the MERIT DEM, and n is the number of observations. The profiles generated from both elevation sources were also used to perform the visual analytics discussed in the results section.

3. Results

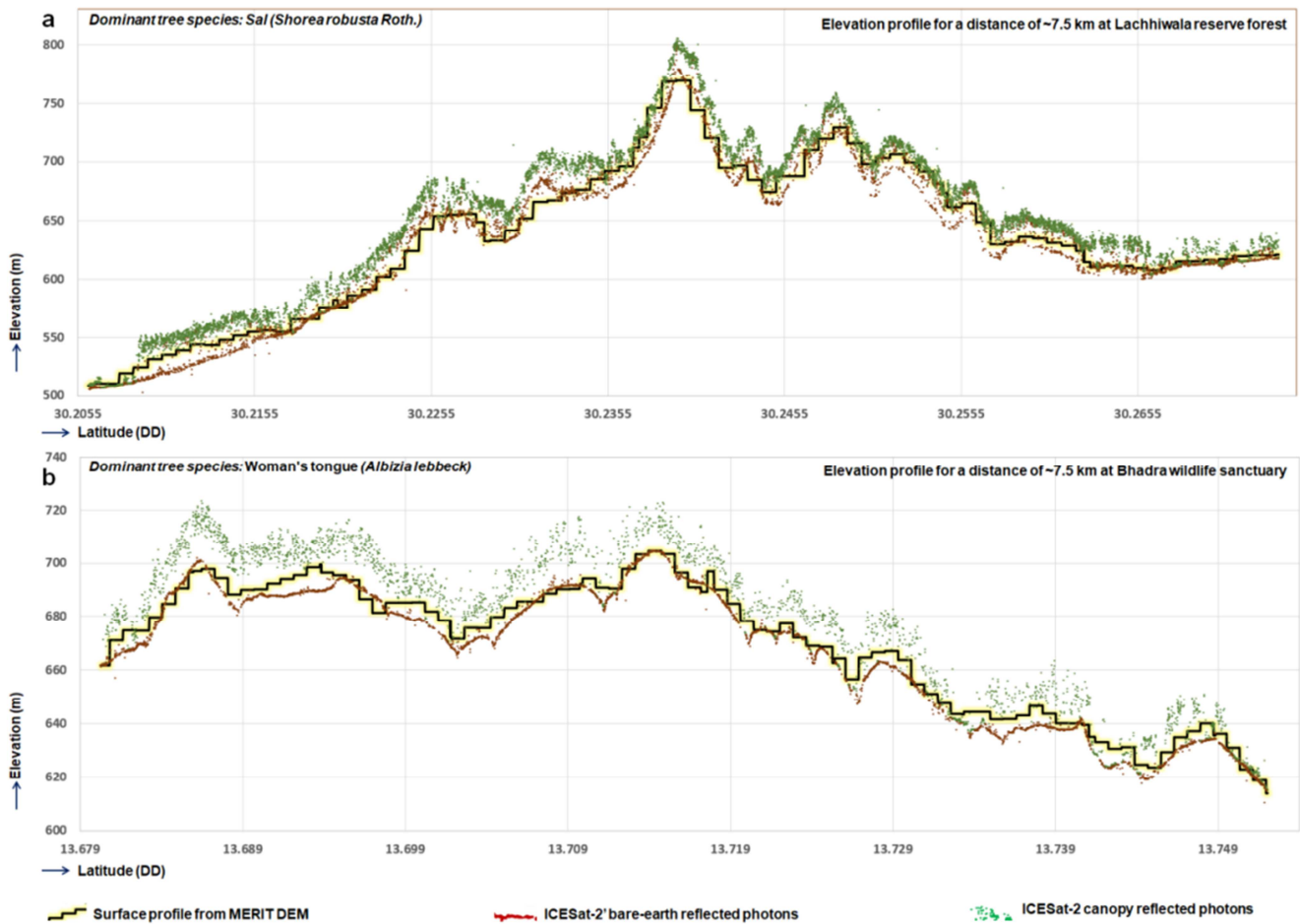


Figure 2. Elevation profiles showing the canopy and ground reflected photons retrieved from the ICESat-2 geolocated photons and corresponding elevation profile retrieved from MERIT DEM. a Elevation profiles for the Lachhiwala Reserve forest test site. b Elevation profiles for the Bhadra wildlife sanctuary test site. Note that the elevations from the MERIT DEM are always lesser than the canopy heights derived from ICESat-2 geolocated photons, which implies the successful implementation of tree-height bias removal.

Figure 2 shows the profiles generated from both elevation sources in the experiment. The profile diagrams contain the Y-axis with the elevation in meters (heights based on the EGM96 vertical datum), and the X-axis has the latitude acquired by the ICESat-2 ground track. Specifically, figure 2a

shows the profiles for the Lachhiwala reserve forest, which is in the elevation range of ~500 to 775 m.a.s.l and the canopy height ranging between 30 to 33 m. Similarly, figure 2b shows the profiles for the Bhadra wildlife sanctuary of Western Ghats in the elevation range between ~620 to 720 m.a.s.l and

the canopy height between 20 to 22 m. The primary observation from the profiles is that the MERIT DEM's implementation of the tree-height bias removal algorithm is successful. This is evident in the profiles of both the study areas (refer to figure 2), wherein the elevations from the MERIT DEM are always lesser than the canopy heights, including those with steep slopes.

The RMSE, MAE, and MBE computed between the elevations retrieved from MERIT DEM and ICESat-2 ground reflected geolocated photons for the Lachhiwala Reserve forest are 10.28 m, 7.78 m, and 0.69 m, respectively, with observations $n=5954$ of ground reflected photons. Similarly, the RMSE, MAE, and MBE values for Bhadra wildlife sanctuary are 4.52 m, 3.82 m, and 3.04 m, respectively, with observations $n=3900$ of ground reflected photons.

4. Discussion

In comparison with the classic pulse-limited altimeters, there are advantages with the ICESat-2 micro-pulse LiDAR (photon-counting) technology; as the photons reflect from the top of the canopy, within the canopy, and the ground, one can perform studies related to vegetation also [56, 57]. In this evaluation procedure, we have taken advantage of this phenomenon to delineate the canopy-reflected and ground-reflected photons that are counted by the ICESat-2's ATLAS sensor (refer to figure 2). In forest regions, the percentage of the number of photons reflecting from the ground depends on the structure of the existing canopy. In this research, for a stretch of 7.5 km individually for the two test sites, elevations from 5954 and 3900 ground reflected photons from the Lachhiwala Reserve forest containing Sal trees and the Bhadra wildlife sanctuary containing *Albizia lebeck* species had been accumulated, respectively. The proven accuracy of elevations from the geolocated photons from ICESat-2 is at the centimeters level [58-60]. Thus, this vast number and highly accurate observations act as qualified reference elevations to validate the MERIT DEM. Earlier, Lian *et al.* [61] suggested using the elevation values from the ground-reflected geolocated photons as control points in remote sensing applications.

Tree-height bias removal from the existing space-borne DEMs (SRTM3 and AW3D DEM) is one of the prime objectives during the generation of the MERIT DEM along with the removal of inaccuracies due to absolute bias, strip noise, and speckle noise. The need to remove tree height bias from the space-borne DEMs can be attributed to the reason that acquisition methods in radar interferometry and optical stereo imagery cannot measure terrain elevations beneath the forest canopies. To remove the tree height bias in MERIT DEM, Yamazaki *et al.* [9] have adopted the methods suggested by Baugh *et al.* [62] and O'Loughlin *et al.* [63]. Accordingly, in the MERIT DEM, the tree height bias was estimated as a tree density and heights function, which was constructed by comparing the DEM, global forest data sets, and ICESat lowest elevations. ICESat is the predecessor mission of ICESat-2, operated from 2003 till 2009 in

campaign modes. The working principles of ICESat are different from the recent ICESat-2, where the Geoscience Laser Altimeter System (GLAS), a sensor on-board ICESat operated at 1064 nm (infrared) to produce non-overlapping and elliptical footprints of ~ 70 m diameters for every 172 m along the track [64, 65].

Through the validation process shown in this research, the Lachhiwala Reserve forest, a dense patchy forest situated on the outer Himalayas, yielded 10.28 m and 7.78 m of RMSE and MAE, respectively. A bare-earth model generated from existing DEMs may accumulate errors from the original DEMs [27]. Generating DEMs for mountainous areas, especially Himalayan-like terrain, is challenging and can induce inaccuracies at steep slopes [66]. Open-access DEMs like SRTM3 and AW3D too consist of inaccuracies in the mountainous topography with steep slopes and can inherit two to three times the same error caused in flat regions [67-70]. During their validation process, Gupta *et al.* [71] reported an error above 70 m in the Himalayan region in SRTM DEM. An RMSE of ~ 10 m obtained in this research for MERIT DEM in the Himalayan terrain with the forested region is a significant improvement over previously available DEMs. Moreover, from figure 2a, it is evident that the elevation from the MERIT DEM is always lesser than the canopy line, which suggests the successful reduction of tree height bias in MERIT DEM. An MBE of ~ 0.69 m for this study region indicates a slight positive bias or overestimation. Thus, there is a scope to decrease the canopy height by the MERIT DEM's tree height removal algorithm, especially at the steep slopes (refer to figure 2a). The inaccuracies reported here concerning the Lachhiwala Reserve forest are well within the MERIT DEM specification, as Yamazaki *et al.* [9] mentioned, specifically for mountainous topographies with steep slopes.

For the study area in the rolling hills of the Western Ghats, i.e., the Bhadra wildlife sanctuary, the RMSE, MAE, and MBE are 4.52 m, 3.82 m, and 3.04 m, respectively. Here too, the elevation profile retrieved from the MERIT DEM is always lesser than the canopy height of the study region (refer to figure 2b), and the accuracies obtained are well within the specification of the MERIT DEM. Moreover, this site's inaccuracies are significantly lesser than the test site falling in the mountainous topography. MERIT DEM, during its generation, utilized the canopy heights from the ICESat mission to reduce the tree-height bias. Earlier investigations done to validate the canopy heights from the ICESat mission reported inaccuracies ranging between 3 to 12 m [72-77], this confirms that the inaccuracies from (earlier) ICESat mission might have propagated in MERIT DEM.

MERIT DEM, considered the best effort in global DEMs to date, was appreciated for its qualities and used as a source to derive a global dataset comprising different geomorphometric features, namely Geomorpho90m, conceptualized and developed by Amatulli *et al.* [15]. Similarly, MERIT Hydro - a global flow direction map at 3-arc seconds was conceptualized and developed by Yamazaki *et al.* [14] by considering MERIT DEM and water body data sets. It is appreciated by the researchers due to its improved accuracy compared to other

open-access DEMs by researchers like Uemaa et al. [4] and Chai et al. [78]. However, its spatial resolution may be a limitation for regional-level applications. Along with improving the spatial resolution, the future version of MERIT DEM can include a tree-height bias removal method in its algorithm by using the canopy heights from the high-resolution lidar data sets available from the ICESat-2 mission.

5. Conclusion

Most geoscientific applications need accurate digital models representing the topography of the Earth's surface. Even though space-borne open-access DEMs are available for the scientific fraternity, they are qualified as DSMs rather than bare-earth models. The need for bare-earth topography is eminent for earth sciences, especially for the applications related to hydrology and disaster-related themes. MERIT DEM is an effort towards representing a bare-earth model. Validation is an essential and scientific process to record the accuracy of a model. This research has validated the MERIT DEM's performance in terms of a bare-earth model. Ground-reflected geolocated photons from the ICESat-2 lidar mission are qualified data sources that can act as reference elevation values. Elevation values from MERIT DEM and ICESat-2 photons were compared in forest regions to check the reliability of the tree-height bias removal algorithm of the former. The two test sites, one located in the mountainous topography and the other in relatively flat terrain, were used to check the performance of the MERIT DEM.

Accuracy quantifiers like RMSE and MAE computed between the elevations retrieved from MERIT DEM and ICESat-2 ground reflected photons for the two study areas were reported. The inaccuracies obtained in this research were well within the accuracy specifications of the MERIT DEM. The reasons for the inaccuracies in the MERIT DEM were also studied and attributed to the usage of tree heights from the coarse resolution lidar data obtained from the ICESat (predecessor version of ICESat-2). Moreover, the visual analytics using the profile diagrams in this research confirm the successful implementation of MERIT DEM's tree-height removal algorithm since the elevations from the MERIT DEM are always lesser than the canopy height of the test sites. However, MAE resulted in a positive bias suggesting further improvement in the algorithm's performance to qualify as a true bare-earth model.

This research proves the significance of validating bare-earth models using the ground-reflected photons from the high-resolution and highly accurate ICESat-2 lidar data. During the generation of MERIT DEM, related error removal algorithms were included to reduce speckle noise, stripe noise, absolute bias, and tree height bias. In this research, we have vested our interest in assessing the tree-height bias only, which is a limitation. The scope of future research can include a comprehensive assessment of MERIT DEM's accuracy by including all the major vertical height error removal

algorithms.

Acknowledgments

The authors gratefully acknowledge the science team of MERIT DEM for providing access to the data. Similarly, the authors sincerely thank the science teams of ICESat-2 for providing access to the original data sources used in this study. This work was conducted with the infrastructure provided by National Remote Sensing Centre (NRSC), for which the authors were indebted to the Chief General Manager of RCs and the Director, NRSC, Hyderabad. We acknowledge the continued support and scientific insights given by Mr. Rakesh Fararoda, Mr. Sagar S Salunkhe, Mr. Manish K Verma, and other staff members of Regional Remote Sensing Centre—West, NRSC/ISRO, Jodhpur.

References

- [1] Zhou QM (2017) Digital elevation model and digital surface model. In Richardson D, Castree N, Goodchild MF, Kobayashi A, Liu W, Marston RA (Eds.), *The international encyclopedia of geography: People, the Earth, environment, and technology*. Wiley-Blackwell, NJ, pp 1–17. <https://doi.org/10.1002/9781118786352.wbieg0768>
- [2] Moudrý V, Lecours V, Gdulová K, Gábor L, Moudrý L, Kropáček J, Wild J (2018) On the use of global DEMs in ecological modelling and the accuracy of new bare-earth DEMs. *Ecol Model* 383: 3-9. <https://doi.org/10.1016/j.ecolmodel.2018.05.006>
- [3] Polidori L, El Hage M (2020) Digital elevation model quality assessment methods: A critical review. *Remote sens* 12 (21): 3522. <https://doi.org/10.3390/rs12213522>
- [4] Uemaa E, Ahi S, Montibeller B, Muru M, Kmoch A (2020) Vertical accuracy of freely available global digital elevation models (ASTER, AW3D30, MERIT, TanDEM-X, SRTM, and NASADEM). *Remote Sens* 12 (21): 3482. <https://doi.org/10.3390/rs12213482>
- [5] Hirt C (2017) Artefact detection in global digital elevation models (DEMs): The Maximum Slope Approach and its application for complete screening of the SRTM v4.1 and MERIT DEMs. *Remote Sens Environ* 207: 27-41. <https://doi.org/10.1016/j.rse.2017.12.037>
- [6] Sampson CC, Smith AM, Bates PD, Neal JC, Trigg MA (2016) Perspectives on open access high resolution digital elevation models to produce global flood hazard layers. *Front Earth Sci* 3: 85. <https://doi.org/10.3389/feart.2015.00085>
- [7] Gallant JC, Read AM, Dowling TI (2012) Removal of tree offsets from SRTM and other digital surface models. *Int Arch Photogramm Remote Sens Spat Inf Sci* 39 (14): 275-280. <https://doi.org/10.5194/ISPRSARCHIVES-XXXIX-B4-275-2012>
- [8] DeWitt JD, Warner TA, Chirico PG, Bergstresser SE (2017) Creating high-resolution bare-earth digital elevation models (DEMs) from stereo imagery in an area of densely vegetated deciduous forest using combinations of procedures designed for lidar point cloud filtering. *GISci Remote Sens* 54 (4): 552-72. <https://doi.org/10.1080/15481603.2017.1295514>

- [9] Yamazaki D, Ikeshima D, Tawatari R, Yamaguchi T, O'Loughlin F, Neal JC, Sampson CC, Kanae S, Bates PD (2017) A high-accuracy map of global terrain elevations. *Geophys Res Lett* 44 (11): 5844-53. <https://doi.org/10.1002/2017GL072874>
- [10] Faherty D, Schumann GJ, Moller DK (2020) Bare earth DEM generation for large floodplains using image classification in high-resolution single-pass InSAR. *Front Earth Sci* 8: 27. <https://doi.org/10.3389/feart.2020.00027>
- [11] Liu Y, Bates PD, Neal JC, Yamazaki D (2021) Bare-Earth DEM Generation in Urban Areas for Flood Inundation Simulation Using Global Digital Elevation Models. *Water Resour Res* 57 (4): e2020WR028516.
- [12] Pimenova O, Roberts C, Rizos C (2022) Regional "Bare-Earth" Digital Terrain Model for Costa Rica Based on NASADEM Corrected for Vegetation Bias. *Remote Sens* 14 (10): 2421. <https://doi.org/10.3390/rs14102421>
- [13] Hawker L, Uhe P, Paulo L, Sosa J, Savage J, Sampson C, Neal J (2022) A 30 m global map of elevation with forests and buildings removed. *Environ Res Lett* 17 (2): 024016. <https://doi.org/10.1088/1748-9326/ac4d4f>
- [14] Yamazaki D, Ikeshima D, Sosa J, Bates PD, Allen GH, Pavelsky TM (2019) MERIT Hydro: a high-resolution global hydrography map based on latest topography dataset. *Water Resour Res* 55 (6): 5053-73. <https://doi.org/10.1029/2019WR024873>
- [15] Amatulli G, McInerney D, Sethi T, Strobl P, Domisch S (2020) Geomorpho90m, empirical evaluation and accuracy assessment of global high-resolution geomorphometric layers. *Sci Data* 7 (1): 162. <https://doi.org/10.1038/s41597-020-0479-6>
- [16] Rizzoli P, Martone M, Gonzalez C, Wecklich C, Tridon DB, Brütigam B, Bachmann M, Schulze D, Fritz T, Huber M, Wessel B (2017) Generation and performance assessment of the global TanDEM-X digital elevation model. *ISPRS J Photogramm Remote Sens* 132: 119-39. <https://doi.org/10.1016/j.isprsjprs.2017.08.008>
- [17] Wessel B (2018) TanDEM-X ground segment-DEM products specification document. Oberpfaffenhofen, Germany: EOC, DLR.
- [18] AIRBUS (2020) Copernicus DEM: Copernicus digital elevation model product hand book Report AO/1-9422/18/I-LG, European Space Agency. https://spacedata.copernicus.eu/documents/20126/0/GEO1988-CopernicusDEM-SPE-002_ProductHandbook_I1.00.pdf.
- [19] Willmott CJ, Matsuura K (2006) On the use of dimensioned measures of error to evaluate the performance of spatial interpolators. *Int J Geogr Inf Sci* 20 (1): 89-102. <https://doi.org/10.1080/13658810500286976>
- [20] Schneider P, Xhafa F (2022) Anomaly detection: Concepts and methods. In: *Anomaly Detection and Complex Event Processing Over IoT Data Streams: With Application to EHealth and Patient Data Monitoring*. Academic Press. pp 49-66. <https://doi.org/10.1016/b978-0-12-823818-9.00013-4>
- [21] Fisher PF, Tate NJ (2006) Causes and consequences of error in digital elevation models. *Prog Phys Geogr* 30 (4): 467-89. <https://doi.org/10.1191/0309133306pp492ra>
- [22] Mesa-Mingorance JL, Ariza-López FJ (2020) Accuracy assessment of digital elevation models (DEMs): A critical review of practices of the past three decades. *Remote Sens* 12 (16): 2630. <https://doi.org/10.3390/rs12162630>
- [23] Höhle J, Höhle M (2009) Accuracy assessment of digital elevation models by means of robust statistical methods. *ISPRS J Photogramm Remote Sens* 64 (4): 398-406. <https://doi.org/10.1016/j.isprsjprs.2009.02.003>
- [24] Liu Z, Zhu J, Fu H, Zhou C, Zuo T (2020) Evaluation of the vertical accuracy of open global DEMs over steep terrain regions using ICESat data: a case study over Hunan Province, China. *Sensors* 20 (17): 4865. <https://doi.org/10.3390/s20174865>
- [25] Vassilaki DI, Stamos AA (2020) TanDEM-X DEM: Comparative performance review employing LIDAR data and DSMs. *ISPRS J Photogramm Remote Sens* 160: 33-50. <https://doi.org/10.1016/j.isprsjprs.2019.11.015>
- [26] Chen W, Yao T, Zhang G, Li F, Zheng G, Zhou Y, Xu F (2022) Towards ice-thickness inversion: an evaluation of global digital elevation models (DEMs) in the glacierized Tibetan Plateau. *Cryosphere* 16 (1): 197-218. <https://doi.org/10.5194/tc-16-197-2022>
- [27] Dandabathula G, Hari R, Ghosh K, Bera AK, Srivastav SK (2022) Accuracy assessment of digital bare-earth model using ICESat-2 photons: analysis of the FABDEM. *Model Earth Syst Environ*. <https://doi.org/10.1007/s40808-022-01648-4>
- [28] Li H, Zhao J, Yan B, Yue L, Wang L (2022) Global DEMs vary from one to another: an evaluation of newly released Copernicus, NASA and AW3D30 DEM on selected terrains of China using ICESat-2 altimetry data. *Int J Digit Earth* 15 (1): 1149-68. <https://doi.org/10.1080/17538947.2022.2094002>
- [29] Neumann TA, Martino AJ, Markus T, Bae S, Bock MR, Brenner AC, Brunt KM, Cavanaugh J, Fernandes ST, Hancock DW, Harbeck K (2019) The ice, cloud, and land elevation Satellite-2 mission: a global geolocated photon product derived from the advanced topographic laser altimeter system. *Remote Sens Environ* 233: 111325. <https://doi.org/10.1016/j.rse.2019.111325>
- [30] Neuenschwander A, Guenther E, White JC, Duncanson L, Montesano P (2020) Validation of ICESat-2 terrain and canopy heights in boreal forests. *Remote Sens Environ* 251: 112110. <https://doi.org/10.1016/j.rse.2020.112110>
- [31] Bhardwaj A (2022) Assessment of FABDEM on the Different Types of Topographic Regions in India Using Differential GPS Data. *Eng. Proc.* 2022, 27 (1): 79; <https://doi.org/10.3390/ecsa-9-13368>
- [32] Xu C, Fu H, Yang J, Wang L (2022) Assessment of the Relationship between Land Use and Flood Risk Based on a Coupled Hydrological-Hydraulic Model: A Case Study of Zhaojue River Basin in Southwestern China. *Land* 11 (8): 1182. <https://doi.org/10.3390/land11081182>
- [33] Liu K, Song C, Ke L, Jiang L, Pan Y, Ma R (2019) Global open-access DEM performances in Earth's most rugged region High Mountain Asia: A multi-level assessment. *Geomorphology* 338: 16-26. <https://doi.org/10.1016/j.geomorph.2019.04.012>
- [34] Guan L, Pan H, Zou S, Hu J, Zhu X, Zhou P (2020) The impact of horizontal errors on the accuracy of freely available Digital Elevation Models (DEMs). *International J Remote Sens* 41 (19): 7383-99. <https://doi.org/10.1080/01431161.2020.1759840>

- [35] Long NQ, Goyal R, Bui LK, Bui XN (2020) Assessment of Global Digital Height Models over Quang Ninh Province, Vietnam. In: Proceedings of the International Conference on Innovations for Sustainable and Responsible Mining, Volume 1. Springer, Cham, pp. 1-12.
- [36] Preeti K, Prasad AK, Varma AK, El-Askary H (2022) Accuracy assessment, comparative performance, and enhancement of public domain digital elevation models (aster 30 m, srtm 30 m, cartosat 30 m, srtm 90 m, merit 90 m, and tandem-x 90 m) using dgps. *Remote Sens* 14 (6): 1334. <https://doi.org/10.3390/rs14061334>
- [37] Archer L, Neal JC, Bates PD, House JI (2018) Comparing TanDEM-X data with frequently used DEMs for flood inundation modeling. *Water Resour Res* 54 (12): 10-205. <https://doi.org/10.1029/2018WR023688>
- [38] Xu K, Fang J, Fang Y, Sun Q, Wu C, Liu M (2021) The importance of Digital Elevation Model selection in flood simulation and a proposed method to reduce DEM errors: A case study in Shanghai. *Int J Disaster Risk Sci* 12: 890-902.
- [39] Garrote J (2022) Free global DEMs and flood modelling—A comparison analysis for the January 2015 flooding event in Mocuba City (Mozambique). *Water* 14 (2): 176. <https://doi.org/10.3390/w14020176>
- [40] Nguyen BQ, Vo ND, Le MH, Nguyen QD, Lakshmi V, Bolten JD (2023) Quantification of global Digital Elevation Model (DEM)—A case study of the newly released NASADEM for a river basin in Central Vietnam. *J Hydrol: Reg Stud* 45: 101282. <https://doi.org/10.1016/j.ejrh.2022.101282>
- [41] Maung WS, Sasaki J (2020) Assessing the natural recovery of mangroves after human disturbance using neural network classification and Sentinel-2 imagery in Wunbaik Mangrove Forest, Myanmar. *Remote Sens* 13 (1): 52. <https://doi.org/10.3390/rs13010052>
- [42] Gautam MK, Tripathi AK, Manhas RK (2011) Assessment of critical loads in tropical sal (*Shorea robusta* Gaertn. F.) forests of Doon valley Himalayas, India. *Water Air Soil Pollut* 218 (1): 235–264. <https://doi.org/10.1007/s11270-010-0638-z>
- [43] Khare S, Latifi H, Ghosh SK (2018) Multi-scale assessment of invasive plant species diversity using Pléiades 1A, RapidEye and Landsat-8 data. *Geocarto Int* 33 (7): 681-98. <https://doi.org/10.1080/10106049.2017.1289562>
- [44] Ramachandra TV, Kamakshi G, Shruthi BV (2004). Bioresource status in Karnataka. *Renew Sust Energ Rev* 8 (1): 1-47. <https://doi.org/10.1016/j.rser.2003.09.001>
- [45] Neumann TA, Brenner A, Hancock D, Robbins J, Saba J, Harbeck K, Gibbons A, Lee J, Luthcke SB, Rebold T, et al (2021) ATLAS/ICESat-2 L2A Global Geolocated Photon Data, Version 5 Boulder, Colorado USA. <https://doi.org/10.5067/ATLAS/ATL03.005>
- [46] Xiang J, Li H, Zhao J, Cai X, Li P (2021) Inland water level measurement from space-borne laser altimetry: Validation and comparison of three missions over the Great Lakes and lower Mississippi River. *J Hydrol* 597: 126312. <https://doi.org/10.1016/j.jhydrol.2021.126312>
- [47] Popescu SC, Zhou T, Nelson R, Neuenschwander A, Sheridan R, Narine L, Walsh KM (2018) Photon counting LiDAR: An adaptive ground and canopy height retrieval algorithm for ICESat-2 data. *Remote Sens Environ* 208: 154-70. <https://doi.org/10.1016/j.rse.2018.02.019>
- [48] Xie H, Sun Y, Xu Q, Li B, Guo Y, Liu X, Huang P, Tong X (2020) Converting along-track photons into a point-region quadtree to assist with ICESat-2-based canopy cover and ground photon detection. *Int J Appl Earth Obs Geoinf* 112: 102872. <https://doi.org/10.1016/j.jag.2022.102872>
- [49] Narine L, Malambo L, Popescu S (2022) Characterizing canopy cover with ICESat-2: A case study of southern forests in Texas and Alabama, USA. *Remote Sens Environ* 281: 113242. <https://doi.org/10.1016/j.rse.2022.113242>
- [50] Jain AK, Murty MN, Flynn PJ (1999) Data clustering: a review. *ACM Comput Surv* 31 (3): 264-323. <https://doi.org/10.1145/331499.331504>
- [51] Mann AK, Kaur N (2013) Review paper on clustering techniques. *Glob J Comput Sci Technol* 13 (5): 43-47.
- [52] Ester M, Kriegel HP, Sander J, Xu X. (1996) A density-based algorithm for discovering clusters in large spatial databases with noise. In *kdd* 96 (34): 226-231.
- [53] Ali T, Asghar S, Sajid NA (2010) Critical analysis of DBSCAN variations. In *International Conference on Information and Emerging Technologies*, IEEE, pp 1-6. <https://doi.org/10.1109/ICIET.2010.5625720>
- [54] Xie C, Chen P, Pan D, Zhong C, Zhang Z (2021) Improved filtering of ICESat-2 lidar data for nearshore bathymetry estimation using sentinel-2 imagery. *Remote Sens* 13: 4303. <https://doi.org/10.3390/rs13214303>
- [55] Huang J, Xing Y, You H, Qin L, Tian J, Ma J (2019) Particle swarm optimization-based noise filtering algorithm for photon cloud data in forest area. *Remote Sens* 11 (8): 980. <https://doi.org/10.3390/rs11080980>
- [56] Herzfeld UC, McDonald BW, Wallin BF, Neumann TA, Markus T, Brenner A, Field C (2013) Algorithm for detection of ground and canopy cover in micropulse photon-counting lidar altimeter data in preparation for the ICESat-2 mission. *IEEE Trans Geosci Remote Sens* 52 (4): 2109-25. <https://doi.org/10.1109/TGRS.2013.2258350>
- [57] Neuenschwander AL, Magruder LA (2019) Canopy and terrain height retrievals with ICESat-2: A first look. *Remote Sens* 11 (14): 1721. <https://doi.org/10.3390/rs11141721>
- [58] Brunt KM, Neumann TA, Smith BE (2019) Assessment of ICESat-2 ice sheet surface heights, based on comparisons over the interior of the Antarctic ice sheet. *Geophys Res Lett* 46 (22): 13072-8. <https://doi.org/10.1029/2019GL084886>
- [59] Wang C, Zhu X, Nie S, Xi X, Li D, Zheng W, Chen S (2019) Ground elevation accuracy verification of ICESat-2 data: A case study in Alaska, USA. *Opt Express* 27 (26): 38168-79. <https://doi.org/10.1364/OE.27.038168>
- [60] Xing Y, Huang J, Gruen A, Qin L (2020) Assessing the performance of ICESat-2/ATLAS multi-channel photon data for estimating ground topography in forested terrain. *Remote Sens* 12 (13): 2084. <https://doi.org/10.3390/rs12132084>
- [61] Lian W, Zhang G, Cui H, Chen Z, Wei S, Zhu C, Xie Z (2022) Extraction of high-accuracy control points using ICESat-2 ATL03 in urban areas. *Int J Appl Earth Obs Geoinf* 115: 103116. <https://doi.org/10.1016/j.jag.2022.103116>
- [62] Baugh CA, Bates PD, Schumann G, Trigg MA (2013) SRTM vegetation removal and hydrodynamic modeling accuracy. *Water Resour Res* 49 (9): 5276-89. <https://doi.org/10.1002/wrcr.20412>

- [63] O'Loughlin FE, Paiva RC, Durand M, Alsdorf DE, Bates PD (2016) A multi-sensor approach towards a global vegetation corrected SRTM DEM product. *Remote Sens Environ* 182: 49-59. <https://doi.org/10.1016/j.rse.2016.04.018>
- [64] Schutz BE, Zwally HJ, Shuman CA, Hancock D, DiMarzio JP (2005) Overview of the ICESat mission. *Geophys Res Lett* 32 (21): L21S01. <https://doi.org/10.1029/2005GL024009>
- [65] Abshire JB, Sun X, Riris H, Sirota JM, McGarry JF, Palm S, Yi D, Liiva P (2005) Geoscience laser altimeter system (GLAS) on the ICESat mission: on-orbit measurement performance. *Geophys Res Lett* 32 (21): L21S02. <https://doi.org/10.1029/2005GL024028>
- [66] Giribabu D, Kumar P, Mathew J, Sharma KP, Murthy YK (2013) DEM generation using Cartosat-1 stereo data: issues and complexities in Himalayan terrain. *Eur J Remote Sens* 46 (1): 431-43. <https://doi.org/10.5721/EuJRS20134625>
- [67] Fujita K, Suzuki R, Nuimura T, Sakai A (2008). Performance of ASTER and SRTM DEMs, and their potential for assessing glacial lakes in the Lunana region, Bhutan Himalaya. *J Glaciol* 54 (185): 220-8. <https://doi.org/10.3189/002214308784886162>
- [68] Kolecka N, Kozak J (2014) Assessment of the accuracy of SRTM C-and X-Band high mountain elevation data: A case study of the Polish Tatra Mountains. *Pure Appl Geophys* 171: 897-912. <https://doi.org/10.1007/s00024-013-0695-5>
- [69] Mukul M, Srivastava V, Jade S, Mukul M (2017) Uncertainties in the shuttle radar topography mission (SRTM) Heights: Insights from the Indian Himalaya and Peninsula. *Sci Rep* 7 (1): 1-0. <https://doi.org/10.1038/srep41672>
- [70] Kramm T, Hoffmeister D (2021) Comprehensive vertical accuracy analysis of freely available DEMs for different landscape types of the Rur catchment, Germany. *Geocarto Int*. <https://doi.org/10.1080/10106049.2021.1984588>
- [71] Gupta RD, Singh MK, Snehmami S, Ganju A (2014) Validation of SRTM X band DEM over Himalayan Mountain. *Int Arch Photogramm Remote Sens Spat Inf Sci* 40 (4): 71.
- [72] Harding DJ, Carabajal CC (2005) ICESat waveform measurements of within-footprint topographic relief and vegetation vertical structure. *Geophys Res Lett* 32 (21). <https://doi.org/10.1029/2005GL023471>
- [73] Lefsky MA, Harding DJ, Keller M, Cohen WB, Carabajal CC, Del Bom Espirito-Santo F, Hunter MO, de Oliveira Jr R (2005) Estimates of forest canopy height and aboveground biomass using ICESat. *Geophys Res Lett* 32 (22). <https://doi.org/10.1029/2005GL023971>
- [74] Hayashi M, Saigusa N, Oguma H, Yamagata Y (2013) Forest canopy height estimation using ICESat/GLAS data and error factor analysis in Hokkaido, Japan. *ISPRS J Photogramm Remote Sens* 81: 12-8. <https://doi.org/10.1016/j.isprsjprs.2013.04.004>
- [75] Fayad I, Baghdadi N, Bailly JS, Barbier N, Gond V, El Hajj M, Fabre F, Bourguin B (2014) Canopy height estimation in French Guiana with LiDAR ICESat/GLAS data using principal component analysis and random forest regressions. *Remote Sens* 6 (12): 11883-914. <https://doi.org/10.3390/rs61211883>
- [76] Pourrahmati MR, Baghdadi NN, Darvishsefat AA, Namiranian M, Fayad I, Bailly JS, Gond V (2015) Capability of GLAS/ICESat data to estimate forest canopy height and volume in mountainous forests of Iran. *IEEE J Sel Top Appl Earth Obs Remote Sens* 8 (11): 5246-61. <https://doi.org/10.1109/JSTARS.2015.2478478>
- [77] Mahoney C, Hopkinson C, Held A, Kljun N, Van Gorsel E (2016) ICESat/GLAS canopy height sensitivity inferred from airborne LiDAR. *Photogramm Eng Remote Sensing* 82 (5): 351-63. [https://doi.org/10.1016/S0099-1112\(16\)82017-0](https://doi.org/10.1016/S0099-1112(16)82017-0)
- [78] Chai LT, Wong CJ, James D, Loh HY, Liew JJ, Wong WV, Phua MH (2022) Vertical accuracy comparison of multi-source Digital Elevation Model (DEM) with Airborne Light Detection and Ranging (LiDAR). In: *IOP Conference Series: Earth and Environmental Science* 2022 Jun 1 (Vol. 1053, No. 1, p. 012025). IOP Publishing. <https://doi.org/10.1088/1755-1315/1053/1/012025>